RETRACTED: The Effect of Vacuum Annealing Temperature on the Properties of AlCrTiSiN Coating Prepared by Arc Ion Plating

Qiang Zhu [1], Yanmei Liu [1,*], Wanqi Cong [2], Dongmei Chang [1], Qixiang Fan [1], Fengting Cao [1] and Tie-Gang Wang [1,*]

1 Tianjin Key Laboratory of High Speed Cutting and Precision Machining, Tianjin University of Technology and Education, Tianjin 300222, China; zq17862002325@163.com (Q.Z.); dm_chang@hotmail.com (D.C.); qxfan@163.com (Q.F.); fengtingcao_88@126.com (F.C.)

2 Department of Mechanical Engineering, University of Technology Sydney, Sydney 2000, Australia; 13073667@student.uts.edu.au

* Correspondence: 13502158936@163.com (Y.L.); tgwang@tute.edu.cn (T.-G.W.); Tel.: +86-22-8818-1083 (T.-G.W.)

Abstract: In order to further improve the mechanical and tribological properties of AlCrTiSiN coating, annealing treatment was carried out in this work. X-ray diffraction (XRD), scanning electron microscopy (SEM), nanoindentation, scratch tester, friction, and a wear tester were used to characterize and explore the effects of annealing temperature on the coating composition, phase component, surface and cross-sectional morphology, and mechanical properties as well as the friction and wear performance of the AlCrTiSiN coatings. The results indicated that after the vacuum annealing the content of amorphous phase decreased and the average size of nanocrystals increased in varying degrees. With the increase in annealing temperature the coating surface became smoother and the cross-section morphology changed little. The coating hardness first increased and then decreased. The adhesion between the coating and substrate decreased after annealing, but the wear resistance was improved. When the annealing temperature was 800 °C, the mechanical properties and wear resistance of the resulting coating were the best. In this case, the coating hardness was 27 GPa, the critical load was 61 N, the friction coefficient was 0.66, and the wear rate was 1.97×10^{-3} $\mu m^3/N \cdot \mu m^{-1}$.

Keywords: AlCrTiSiN coating; vacuum annealing; mechanical property; tribological performance

1. Introduction

Cutting tools often fail due to poor mechanical properties, wear, and high temperature oxidation. Compared with the development of new materials to prepare a tool base, a hard and tough protective coating on the tool surface can effectively improve the tool surface performance and economic benefits [1–3]. As the typical representative of transition metal nitride coatings, the research on TiN and CrN coatings started early and the technology is mature. Because of excellent hardness and wear resistance, they are widely used in machining, decoration, and other industries [4–8]. The appearance of TiN-coated cutting tools brings great convenience and benefits to society. However, with the development of modern industry people are putting forward more requirements for high efficiency, and a high degree of precision in coated tools, high-speed heavy load cutting, and green dry machining technology have gradually become mainstream in society [9,10]. The thermal stability of TiN-coated tools is greatly tested by high-speed cutting conditions up to 800 °C. TiAlN coating based on TiN coating has excellent high-temperature oxidation resistance (900 °C). The shear strength and compressive strength of the coating can be effectively improved by increasing the Al content in the coating, and the overall mechanical properties can be further improved [11]. Doping Si and Cr elements into the coating can effectively improve the mechanical, friction, and high temperature resistance properties of

the coating [12,13]. Chang et al. [14] prepared AlTiN and AlTiSiN coatings by an acathodic arc deposition system and compared them. It was found that the coating structure became smoother and more compact after Si doping; moreover, the mechanical and tribological properties of the coating were greatly improved. The TiAlCrN coating prepared by Ru et al. [15] by arc ion plating technology showed an NaCl face-centered cubic structure; the outer layer was rich in Al_2O_3 and the inner layer was rich in Cr_2O_3 + TiO_2 under high temperature oxidation conditions, which greatly improved the oxidation resistance of the coating. Fu et al. [16] prepared CrAlTiN and CrAlTiSiN coatings by multi arc ion plating technology. The comparative study found that the mechanical properties of the CrAlTiSiN coatings increased significantly, and the cutting properties were further improved. The cutting performance of the CrAlTiSiN superlattice tool coating prepared by Niu et al. [17] was significantly higher than that of the AlCrN-coated tool.

Thermal stability is an important index for the long-term service of coatings, and many coated parts cause local excessive temperature due to friction. If the thermal stability of the coating is weak, the service life of the workpiece will be greatly reduced. The subsequent heat treatment of the deposited coating at an appropriate temperature can effectively release the residual stress, reduce the internal defects, homogenize the internal elements, and further improve the performance of the coating [18,19].

Forsen et al. [20] studied the decomposition and phase transformation of TiCrAlN coatings at different annealing temperatures. The results showed that the splitting of diffraction peaks and the appearance of h-AlN in TiCrAlN coating with higher Al content were both at a higher vacuum annealing temperature. The hardness of the TiAlN coating decreased rapidly when the annealing temperature exceeded 950 °C, while the hardness of the TiAlN coating remained high when the annealing temperature increased to 1100 °C after doping the Cr element. Zhang et al. [21] carried out vacuum heat treatment on the TiAlSiN coating. The results showed that properly increasing the annealing temperature can effectively promote atomic diffusion and increase the density of the coating. When the annealing temperature was 800 °C, it was found that the amorphous crystal structure appeared near the surface of the TiAlSiN coating, the nanohardness and adhesion reached the maximum value, and the wear resistance was the best. Flink et al. [22] annealed the TiAlSiN coating at 800–1000 °C. During the process, h-(Al,Ti,Si)N gradually transformed into c-TiN and the remaining h-(Al,Ti,Si)N through nucleation and growth. Compared with the original coating, the grain of the $(Ti_{0.33}Al_{0.67})_{0.91}Si_{0.09}N$ coating was refined after annealing, and the hardness was 30.1 ± 2.7 and 28.7 ± 2.4 GPa at 900 and 1000 °C, respectively, which was significantly higher than that in the deposited state (23.6 ± 1.1 GPa). Zhang et al. [23] studied the effect of annealing temperature on the properties of CrAlSiN superlattice coating. The results showed that the fcc-CrN/h-(Al, Si)N structure of the coating remained unchanged when the annealing temperature was 900 °C. When the annealing temperature was further increased to 1100 °C, h-(Al, Si)N decomposed into h-AlN and n-Si_3N_4 and the hardness of the coating decreased obviously.

At present, there are few reports on the preparation and subsequent treatment of AlCrTiSiN coating. Therefore, the AlCrTiSiN coating was prepared by arc ion plating and was annealed in a vacuum; the optimum annealing temperature was obtained; and the effects of annealing temperature on the phase composition, mechanical properties, and tribological properties of the coatings were systematically summarized. After annealing at 800 °C, the mechanical properties and wear resistance of the coating were significantly improved, and the hardness and wear rate were 27 GPa and 1.97×10^{-3} $\mu m^3/N \cdot \mu m^{-1}$, respectively. The treated coating can be widely used for tool surface protection.

2. Experimental Details

2.1. Experimental Materials and Annealing Experiment

Arc ion plating is based on an improved and developed version of evaporation and sputtering coating technology [24]. Compared with magnetron sputtering technology, this has the advantages of high energy, high deposition rate, and high adhesion of the prepared

coating. Therefore, arc ion plating was used in the preparation of the AlCrTiSiN coating. Superalloy (25 mm × 25 mm × 1.5 mm), cemented carbide (30 mm × 30 mm × 3.0 mm), and a monocrystalline silicon wafer (30 mm × 30 mm × 0.67 mm) were chosen as substrate materials. The surface quality of all substrates reached mirror-polished, and their roughness was less than 100 nm, which was measured by a profilometer (D-300, KLA Tencor, Shanghai, China). The samples were placed in acetone, deionized water, and alcohol, respectively, for ultrasonic cleaning for 20 min, and then dried. The samples were placed on the sample holder of the vacuum chamber. The background vacuum was pumped to 3.0×10^{-3} pa and heated to 450 °C for glow and bombardment cleaning. In order to improve the adhesion between the coating and the substrate, CrN was prepared as the transition layer. Finally, AlCrTiSiN coatings were prepared in N_2 (99.999%) + Ar (99.999%). The oxidation resistance of the coating can be improved by properly increasing the Al content in the coating. During the coating process, two targets (Al:Cr:Si = 6:3:1 and Al:Ti:Si = 6:3:1) were chosen to work together. The specific deposition parameters are shown in Table 1.

Table 1. Deposition parameters of the AlCrTiSiN coatings prepared by the arc ion plating.

Parameter	Values
Base pressure (Pa)	3.0×10^{-3}
Deposition pressure (Pa)	3.0×10^{-1}
Deposition temperature (°C)	450
Deposition pressure (Pa)	2.8
Bias voltage (V)	−100
Arc current of Cr cathode (A)	90
Arc current of AlCrSi cathode (A)	100
Arc current of AlTiSi cathode (A)	80
Ar:N_2 gas flow ratio (sccm)	1:12
Substrate rotation speed (r·min^{-1})	40
Deposition time(min)	180
Distance between the target and substrate (mm)	285

Because C, CO, and W elements in the cemented carbide matrix are easy to diffuse into the coating at high temperature, the mechanical properties of the coating are greatly reduced [25]. Therefore, in this vacuum annealing experiment samples of superalloy and a single crystal silicon wafer with AlCrTiSiN coating were placed in a ceramic crucible and fixed in a vacuum tube furnace (TL1200 type, Muffle, Tianjin, China). Firstly, the vacuum degree was pumped to 3.0×10^{-3} pa, then the control program was raised to the set temperature at the heating rate of 10 °C/min for 1 h. Finally, it was cooled to room temperature at the cooling rate of 4 °C/min. The specific experimental parameters are shown in Table 2.

Table 2. Vacuum annealing parameters of the AlCrTiSiN coatings.

Parameters	Values
Base pressure (Pa)	3.0×10^{-3}
Insulation pressure (Pa)	$<1.5 \times 10^{-3}$
Annealing temperature (°C)	600/700/800/900
Heating rate (°C·min^{-1})	10
Heat preservation time (min)	60

2.2. Structure Characterization and Performance Test

Phase identification and microstructure analysis of the AlCrTiSiN coating were carried out by X-ray diffraction (XRD, XPERT-PRO, PANalytical, Almelo, The Netherlands) with monochromatic Co Kα (λ = 1.79021 Å) radiation operated at 35 kV and 50 mA. The analyzed range of diffraction angle 2θ was between 40° and 75°. The surface and cross section morphology of the AlCrTiSiN coating were observed by a scanning electron micro-

scope (SEM, SU8010, Hitachi, Tokyo, Japan). The surface roughness of the coatings was measured by the surface profilometer. The coating composition was determined by an energy-dispersive spectrometer (EDS, GENESIS, EDAX, Philadelphia, America). A nano indentation instrument (TTX NHT-3, Anton Paar, Graz, Austria) was used to repeatedly test the hardness of the coatings before and after annealing, and an average of ten measurements was taken as the final hardness value. A holding time of 10 s and a load of 10 mN were applied. The trihedral Berkovich diamond tip with diameter of 200 μm was used for the indentation test. Before the test, the diamond tip was calibrated with a standard Si sample. The smooth and flat positions were chosen to test, and the distance between the indentations was more than three times the diagonal length of the indentations. In order to avoid the influence of the substrate effect on the hardness measurement value, the indentation depth was less than 1/10 of coating thickness. The scratch tester (RST-3, Anton Paar, Graz, Austria) was used to scratch the coating under 80 N load, and the L_{C2} value was used to characterize the adhesion between the coating and the substrate. The high temperature friction and a wear test machine (THT, Anton Paar, Graz, Austria) were used to test the friction and wear of the wear pair (Al_2O_3 ball) with the hardness of 22 ± 1 GPa. The wear test was carried out at 22 ± 3 °C; the friction radius was 8 mm and the applied external force load was 4 N. Profilometer (D-300, KLA Tencor, Shanghai, China) was used to measure the cross-sectional area of the corresponding coating after the friction test, and then the wear rate of the coating was obtained according to the formula V = A/n·F, where V is the wear rate, A is the cross-sectional area of worn scar, n is the number of friction cycles, and F is the normal load. In order to analyze the wear mechanism of the coating, the wear scar morphology of the coating was obtained by using a depth-of-field optical microscope (VHX-1000C, Keyence, Osaka, Japan).

3. Results and Discussion

3.1. Composition and Phase Constituents

Table 3 shows the element composition of the AlCrTiSiN coatings as deposited and after annealing at 800 °C. It can be seen that the coating composition remains basically unchanged before and after annealing. Both coatings contain Al, Cr, Ti, Si, and N elements. The content of Al and N in the coatings is the highest, about more than 30 at.%. changes; the content of Ti and Cr is relatively low, about 10 at.%; and the content of Si is the lowest, less than 10 at.%. The proportion of Al, Ti, Cr, and Si in the coatings is different from that in the target, which was attributed to the different sputtering yields of each element in reactive sputtering.

Table 3. Composition of the AlCrTiSiN coatings before and after annealing (at.%).

Status	Al	Cr	Ti	Si	N
As-deposited	33.81	9.57	14.58	8.63	33.41
Annealing at 800 °C	34.95	10.91	14.92	6.75	32.47

Figure 1 shows the XRD patterns of the AlCrTiSiN coatings before and after annealing. The diffraction peaks of Si simple substance and its compounds were not detected; they may have existed in the amorphous phase, because the crystallization temperature of Si_3N_4 generally exceeds 1000 °C [26]. It can be seen from the figure that the components of the AlCrTiSiN coatings remained the same before and after annealing, but the diffraction peaks of the coatings gradually became stronger as the annealing temperature rose, which indicates that the coating crystallinity increased after annealing. All the coatings are composed of $AlTi_3$, $Ti_{0.76}N$, Al_5Ti_2, $TiSi_2$, Al_3Ti, and $Al_{0.5}Cr_3Si_{0.5}$ phases, and most of the metal ions were not fully nitride due to the limited N_2 flow in reactive sputtering. As a result, some Al-dominated intermetallic compounds with high hardness and good wear resistance were formed. In addition, a certain amount of N element which could not be detected by XRD may have existed in the amorphous phase.
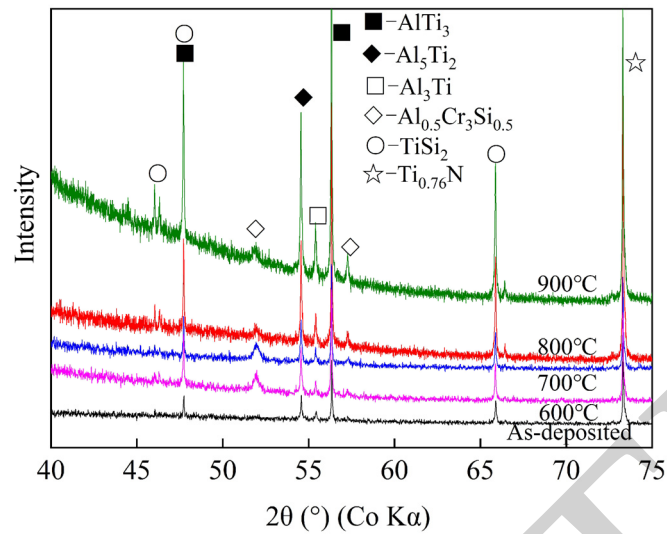
Figure 1. XRD patterns of the AlCrTiSiN coatings before and after annealing at different temperatures.

In order to quantitatively analyze the grain size of the coatings, the average grain size (Ra) of a deposited and annealed AlCrTiSiN coating was calculated according to the strongest diffraction peak of the $AlTi_3$ phase in XRD patterns and Scheler's Formula (1), where λ is the diffraction wavelength of $K\alpha$—Co ray, with a value of 1.79021 Å; B is the half height width of diffraction peak; and θ is the Bragg angle of the corresponding diffraction peak. It can be seen from Figure 2 that the grain size of the $AlTi_3$ phase after annealing was increased compared with that of the as-deposited coating. When the annealing temperature was 900 °C, the grain size of the $AlTi_3$ phase increased to 101.2 nm, which was due to the accelerated diffusion of the grain boundary during the heating process.
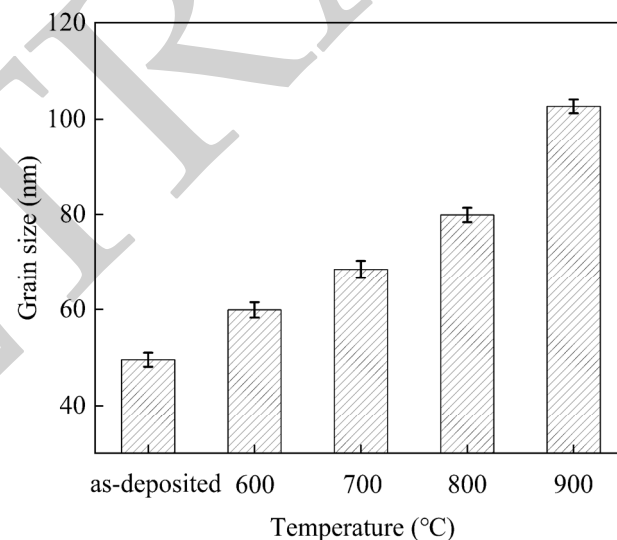
$$Ra = K\lambda/Bcos\theta \tag{1}$$

Figure 2. Average grain size of the $AlTi_3$ phase in the AlCrTiSiN coatings before and after annealing at different temperatures.

3.2. Morphologies

Annealing treatment can change the defect density and microstructure of the coating. Figure 3 shows the surface morphology of the AlCrTiSiN coating as deposited and after vacuum annealing at different temperatures. It can be seen from the figure that there are many particles with different sizes on all the coating surfaces, which is the preparation feature of arc ion plating. With the increase in annealing temperature, the surface roughness of

the coating decreases gradually, as shown in Figure 4, and when the annealing temperature is 900 °C, the number of large particles on the coating surface decreases significantly, which was consistent with the results of Chen et al. [27] This is because the melting point of Al is low (660 °C). With the increase in annealing temperature, some macroparticles with a low melting point melted on the coating surface, which reduced the coating roughness, and some cavities and other defects disappeared [28].
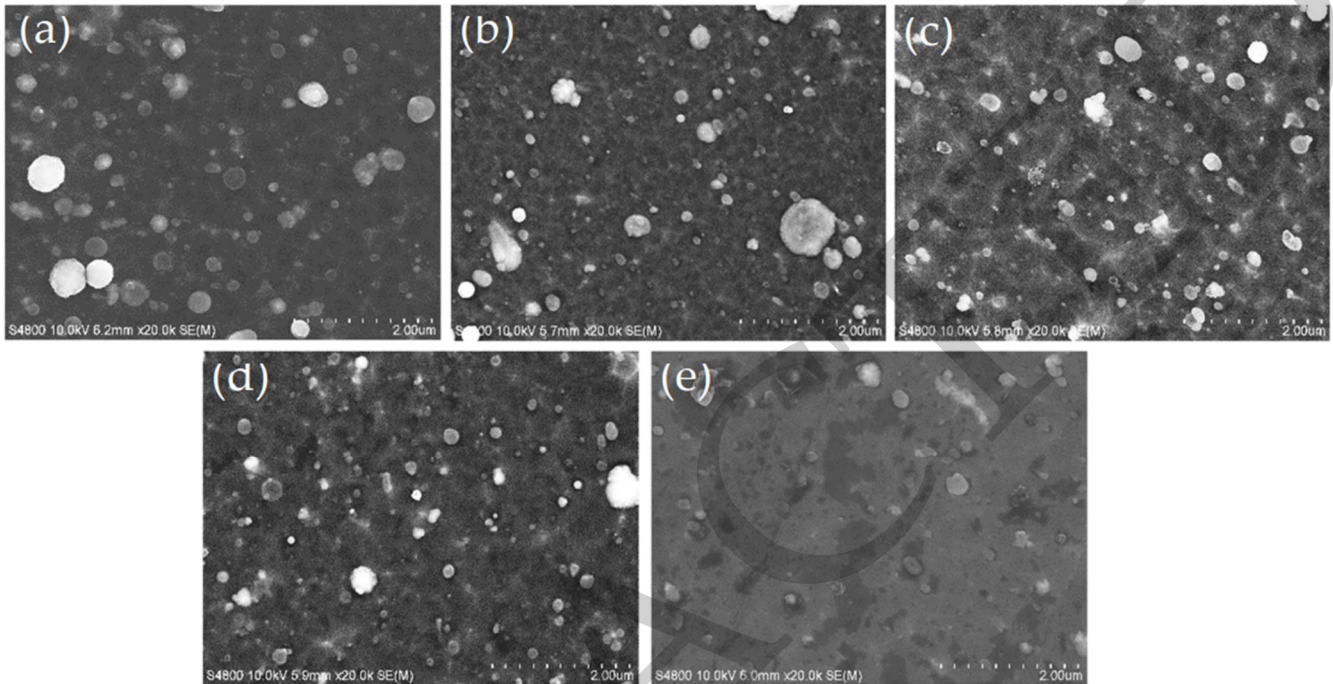

Figure 3. Surface morphologies of the AlCrTiSiN coatings before and after annealing. (**a**) as-deposited, annealed at (**b**) 600 °C, (**c**) 700 °C, (**d**) 800 °C, (**e**) 900 °C.
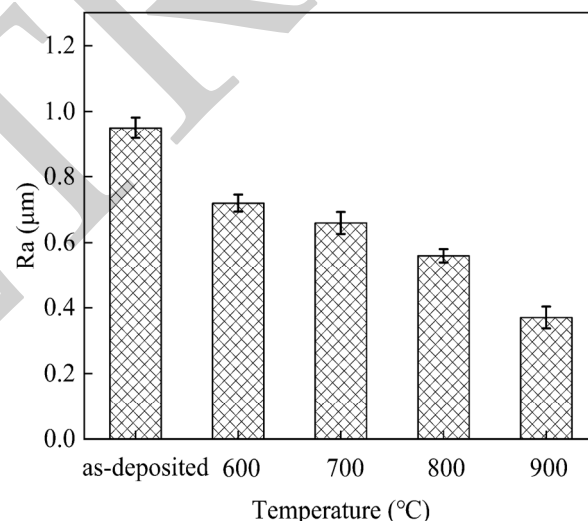

Figure 4. Surface roughness of the AlCrTiSiN coatings before and after annealing at different temperatures.

Figure 5 shows the cross-sectional morphology of the AlCrTiSiN coating as deposited and annealed at 800 °C. It can be seen from the figure that the structure of the coating annealed at 800 °C has no obvious change and still showed no characteristic growth structure, indicating that the coating had high-temperature resistance. Compared with Figure 5a,b, the film substrate interface of AlCrTiSiN coating is smooth after vacuum heat

treatment. This was due to the fact that the energy of the particles in coating increases and the thermal movement was intense at a higher temperature, which resulted in the diffusion between CrN and AlCrTiSiN layers.
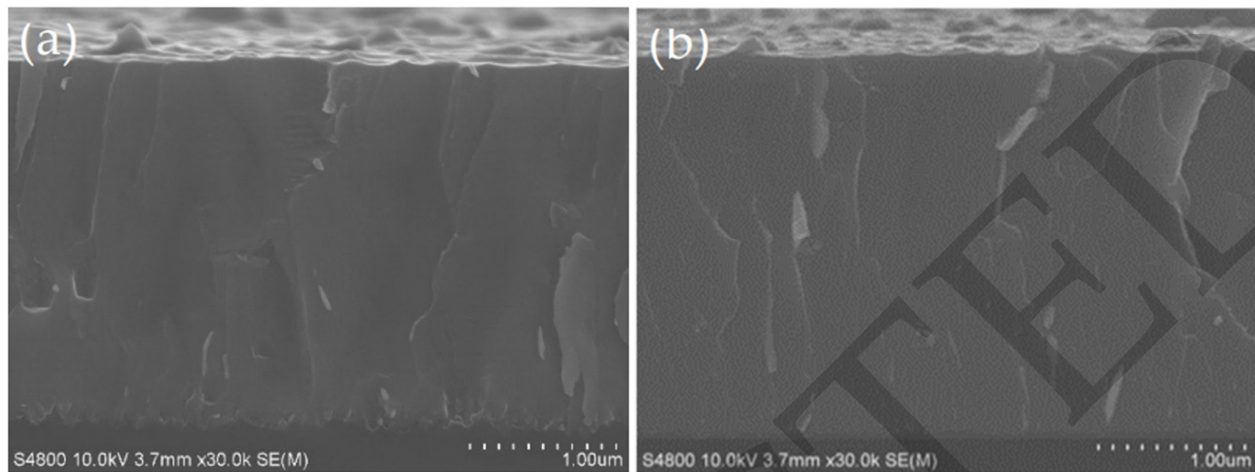

Figure 5. Cross-section morphologies of the AlCrTiSiN coatings before and after annealing, (**a**) as-deposited, (**b**) annealed at 800 °C.

3.3. Mechanical Properties

Figure 6 shows the nanohardness of the AlCrTiSiN as-deposited coating and annealed coating at different temperatures. It can be seen from the figure that the coating hardness firstly increased gradually with the increase in annealing temperature. When the annealing temperature arrived at 800 °C, the resulted coating possessed the maximum hardness of 27 Gpa. On the one hand, the higher annealing temperature enhanced the diffusion ability of atoms in the coating, which made it easy to fill the gap vacancy in the coating and to compact the coating structure. As a result, the atomic migration movement was intensified and the micro uniformity of the coating was improved, which was conducive to an increase in the coating hardness [21,29]. On the other hand, according to the research by Huang [30], Ashith [31], and Meng [32], the partial amorphous phase in the coating could crystallize after annealing, and the content of hard phase increased, which also helped improve the coating hardness. When the annealing temperature was further increased to 900 °C, the the hardness of the resulting coating decreased sharply to the lowest value of 22.3 GPa, which was attributed to an increase in grain size in the coating.
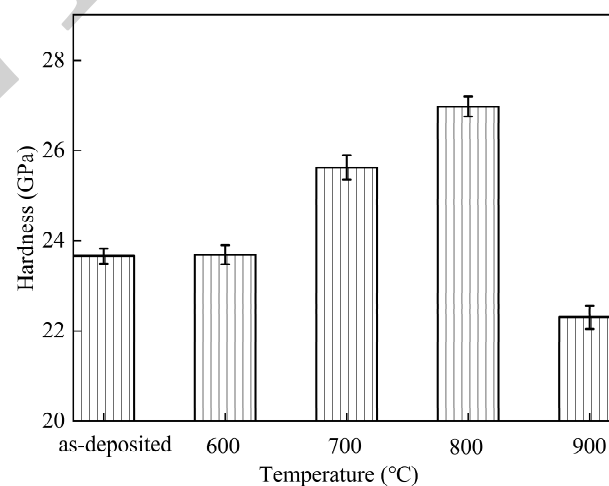

Figure 6. Nanohardness of the AlCrTiSiN coatings before and after annealing at different temperatures.

At present, the scratch method is widely used in related fields, and L_{C2} is used to characterize the adhesion between coating and substrate. Figure 7 shows the change curve of the critical load of the AlCrTiSiN coating in its original state and at different annealing temperatures. The values are all the average values of L_{C2} in each sample. It is well known that proper residual compressive stress is beneficial to improve the adhesion between coating and substrate; however, the deposition residual stress of the coating was released after vacuum heat treatment, and the adhesion between coating and substrate decreased significantly; the critical load of as-deposited coating was 82.1 N. As mentioned above, vacuum annealing can improve the density of the coating, greatly reduce the internal voids, and improve the adhesion between the coating and the substrate. Therefore, with the increase in annealing temperature, the critical load increased gradually. When the temperature was further increased to 900 °C, the grains inside the coating grew further. When the coarse grains were subjected to large shear stress and compressive stress, extrusion stress occurred between the grains, which led to transgranular fracture, which was not conducive to the improvement of the mechanical properties of the coating [33]. In addition, the critical load of the coating was at a high level as a whole. Due to the inherent advantages of high energy of arc ion plating, the coating prepared by this method has a higher critical load than other technologies. Figure 8 shows the scratch morphology of the corresponding AlCrTiSiN coating before and after annealing. It can be seen from Figure 8f that there is a fish scale crack in the scratch, which was due to the plastic deformation of the coating against external force load. This stage did not appear in the coating scratch after annealing, indicating that the adhesion between the coating and substrate decreased.
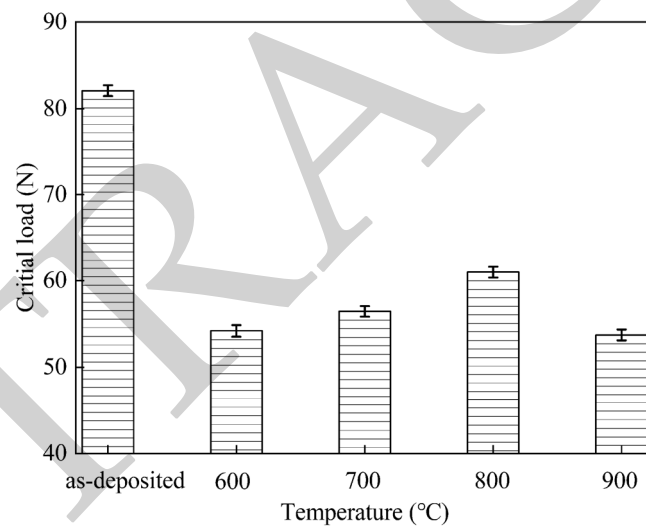

Figure 7. Critical load of the AlCrTiSiN coatings before and after annealing at different temperatures.
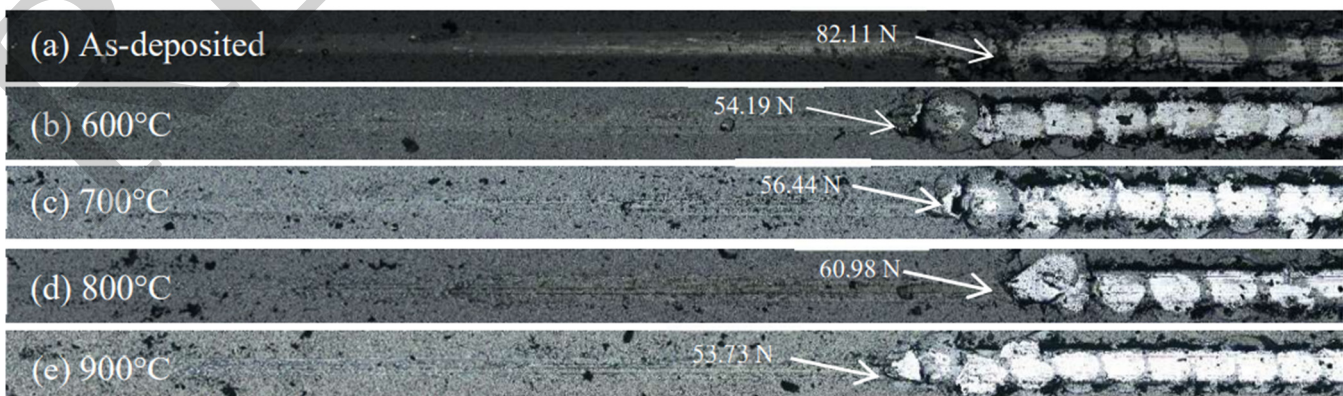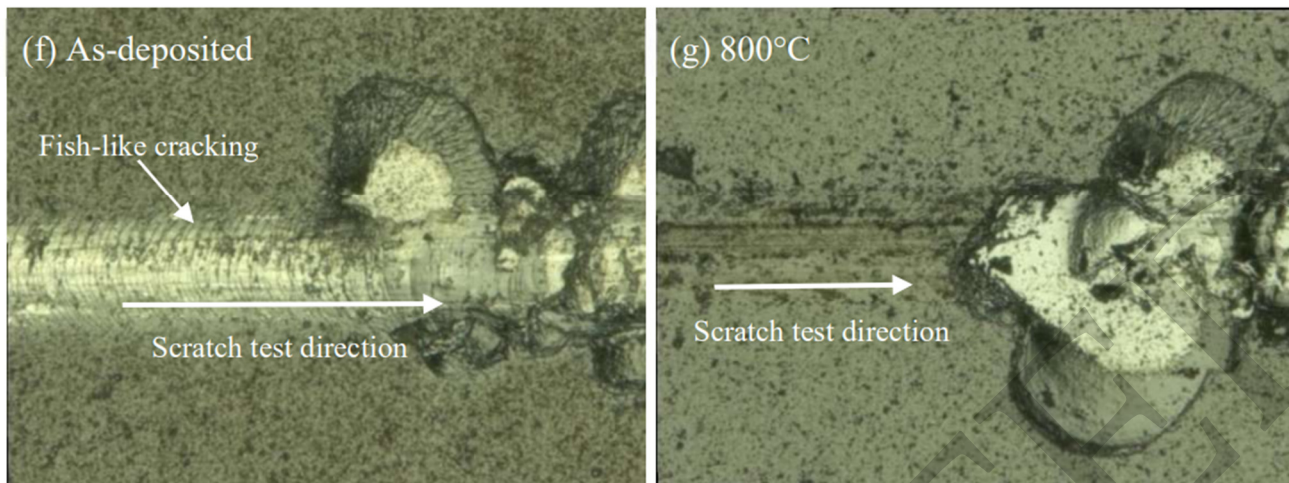

Figure 8. *Cont.*

Figure 8. Scratch morphologies of the AlCrTiSiN coatings before and after annealing: (**a**) the range of normal load is 0–120 N, (**b**–**e**) the range of normal load is 0–80 N; locally amplified scratch morphologies (**f**) as deposited, (**g**) annealed at 800 °C.

3.4. Tribological Behaviors

Figure 9 shows the average friction coefficient of the AlCrTiSiN coatings before and after annealing at different temperatures. They varied in the range of 0.66–0.69, and no obvious difference could be observed. The as-deposited coating possessed the lowest friction coefficient of 0.66. When the annealing temperature was 600 °C, the friction coefficient of the resulting coating was 0.69. In the above two cases, the coating hardness was relatively low, which would increase the contact area of the friction interface. However, the variation in surface residual stress after annealing would also affect the friction coefficient to some extent. When the annealing temperature was further increased to 700 and 800 °C, the porosity in the coating decreased, the density was improved, and the friction coefficient was stabilized at about 0.66. Although the coating hardness was high, the contact area of friction interface was small. When the annealing temperature was further increased to 900 °C, the nanocrystals were too large, which led to a sharp decrease in coating hardness. Similarly, this would increase the contact area of the friction interface and slightly increase the friction coefficient.
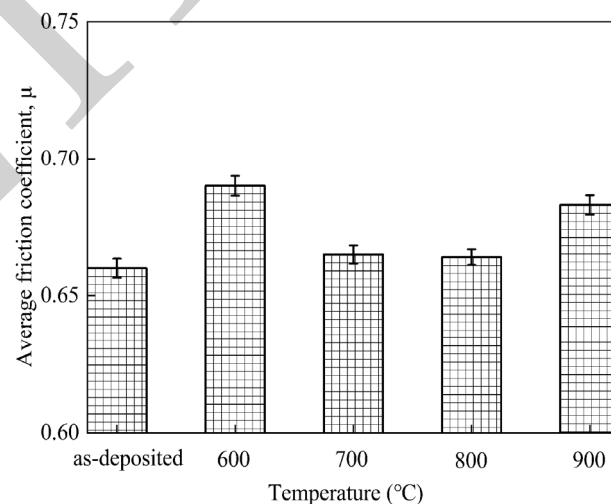

Figure 9. Friction coefficient of the AlCrTiSiN coatings before and after annealing at different temperatures.

Figure 10 shows the wear rate of the AlCrTiSiN as-deposited coatings and vacuum annealed coatings at different temperatures. It can be seen from the figure that the wear rate

of the as-deposited coating was about 1.97×10^{-3} $\mu m^3/N \cdot \mu m^{-1}$. After annealing, the wear resistance of the resulting coatings was improved significantly. The reason for this was that at high annealing temperature the diffusion ability of atoms in the coating was enhanced, especially for the N atoms with small radius, which filled in the internal defects of the coating and made the coating more compact so as to reduce the surface roughness of the coating. Therefore, the contact stress between the friction pair was reduced and the third body wear phenomenon was improved. As we know, the hardness of the coating directly affected the contact area of friction interface, so it also affected the wear resistance of the coating. As mentioned above, annealing at an appropriate temperature would reduce the content of the amorphous phase in the coating, increase the average size of the nanocrystals, and improve their hardness, which helped improve the wear resistance of the coating [31]. Although the coating hardness after annealing at 600 °C was lower than that of coating annealed at 700 and 800 °C, the wear rates of the three coatings were similar, which may be due to the variation of residual stresses during annealing treatment. When the annealing temperature rose to 900 °C, the wear resistance of the resulting coating was weakened due to its lower hardness.
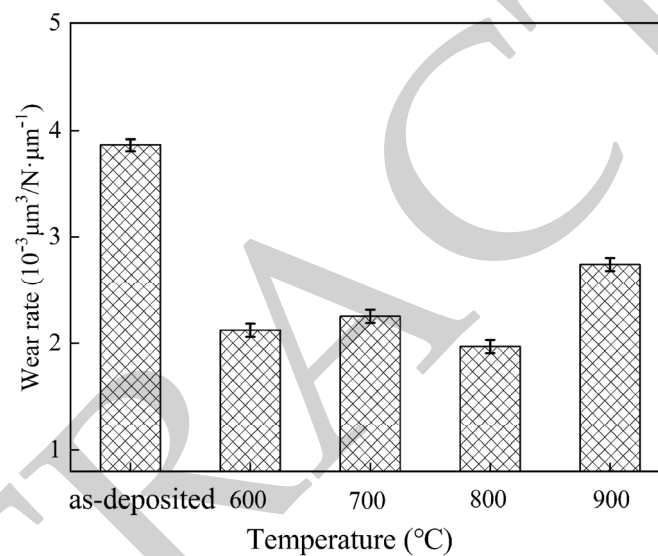

Figure 10. Wear rate of the AlCrTiSiN coatings before and after annealing at different temperatures.

Figure 11 shows the wear morphologies of the AlCrTiSiN coatings before and after annealing at different temperatures. It was obvious that the width of worn scar in as-deposited coating was the largest; the reason was that the hardness of as-deposited coating was the lowest, and the contact area between the Al_2O_3 ball and the coating was large, which accelerated the wear of the coating. In contrast, after annealing at 600 and 700 °C, the hardness and density of the coating increased, which slowed down the wear of the coating, and the wear width was narrow. When the annealing temperature rose to 800 °C, the wear rate of the coating was the lowest and the wear width was relatively wide. This was because the hardness of the coating was the highest and the friction wear of the wear pair was intensified after many cycles; thus, the contact area between the friction pair and the coating increased, leaving a wide wear mark. Through careful observation, it was found that there are micro furrows in all the wear marks, which was due to the coating particles falling off and participating in the friction, resulting in abrasive wear. The residual blue and dark debris in the wear marks indicated that there was oxidation wear in the friction process. Moreover, the largest amount of wear debris remains in Figure 11e, indicating that the oxidation wear of the coating was intense and the wear resistance was reduced at this annealing temperature. This was due to the release of the internal compressive stress of the coating at high annealing temperature, and the poor mechanical properties of the coating at this time are not conducive to the improvement of the wear resistance of the coating.

The worn morphology and EDS analysis of the AlCrTiSiN coating annealed in vacuum at 800 °C are shown in Figure 12. The results showed that the atomic fractions of the chemical elements in the test area are Al 21.4%, Cr 14.61%, Ti 9.21%, Si 3.39%, O 36.24%, and N 15.15%. All these were elements in the coating, and no metal elements in a superalloy substrate (Co, Mo, W, et al.) were found, which indicated that the coating was not worn through. The test area contained a lot of O elements, which was due to the formation of oxides at friction interface during the friction process, indicating that the coating wear mechanism included oxidation wear [34].
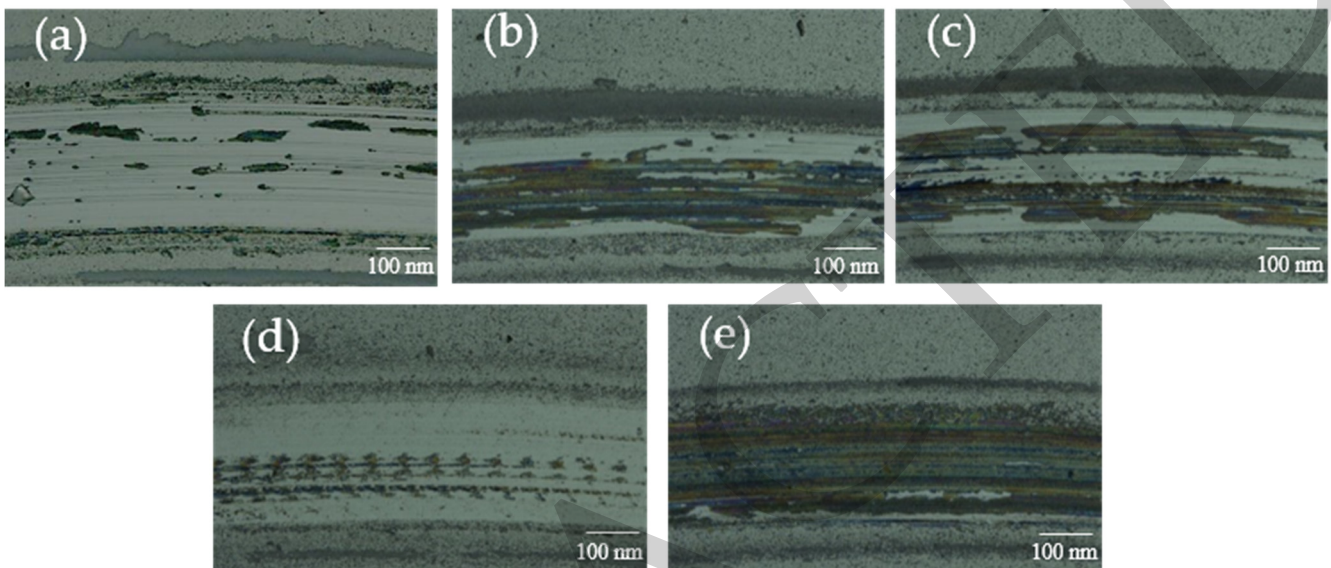

Figure 11. Wear morphologies of the AlCrTiSiN coatings before and after annealing. (**a**) as-deposited, annealed at (**b**) 600 °C, (**c**) 700 °C, (**d**) 800 °C, (**e**) 900 °C.
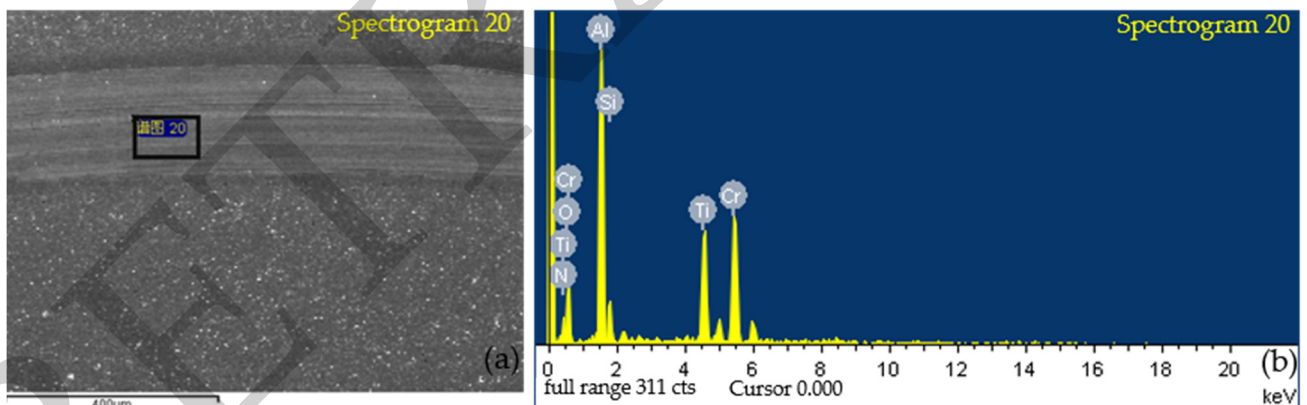

Figure 12. SEM morphology and EDS analysis of the worn scar for the AlCrTiSiN coating after annealing at 800 °C. (**a**) SEM morphology, (**b**) EDS test chart.

4. Conclusions

In this work the microstructure, composition, and mechanical and tribological properties of AlCrTiSiN coatings before and after annealing were studied. Some important conclusions were drawn:

(1) After vacuum annealing, the average size of nanocrystals showed a clear upward trend with the increase in annealing temperature. When the annealing temperature was 900 °C, the maximum grain size was 101.2 nm.

(2) With the increase in annealing temperature, the surface roughness of the coating decreased, and when the annealing temperature was 900 °C, the quantity and size of

macroparticles on the surface decreased significantly. The coating microstructure had no obvious change before and after annealing.

(3) The comprehensive properties of AlCrTiSiN coating were improved after the vacuum annealing treatment. The mechanical properties and wear resistance of the AlCrTiSiN coating were the best when the annealing temperature was 800 °C. In this case, the coating hardness was 27 GPa, the critical load was 61 N, the friction coefficient was 0.66, and the wear rate was 1.97×10^{-3} $\mu m^3/N \cdot \mu m^{-1}$.

(4) After annealing at 800 °C, the hardness and tribological performance of the AlCrTiSiN coatings were slightly inferior to those of the TiAlSiN coatings prepared by Zhang et al. [21], so the preparation technology and heat treatment process of the AlCrTiSiN coatings were expected to be further optimized.

Author Contributions: Conceptualization, Q.Z. and Y.L.; methodology, D.C.; validation, Q.F., F.C. and T.-G.W.; formal analysis, Q.Z.; investigation, Q.Z. and Y.L.; resources, Q.F.; data curation, Q.Z.; writing—original draft preparation, W.C.; writing—review and editing, W.C.; supervision, T.-G.W.; project administration, T.-G.W.; funding acquisition, T.-G.W. All authors have read and agreed to the published version of the manuscript.

Institutional Review Board Statement: Not applicable.

Informed Consent Statement: Not applicable.

Data Availability Statement: Not applicable.

Conflicts of Interest: The authors declare no conflict of interest.

References

1. Volosova, M.; Vereschaka, A.; Andreev, N.; Sotova, C.; Bublikov, J. Improvement of the performance properties of cutting tools using the multilayer composite wear-resistant coatings based on nitrides of Cr, Mo, Zr, Nb, and Al. *Mater. Today Proc.* **2021**, *38*, 1421. [CrossRef]
2. Al-Tameemi, H.A.; Al-Dulaimi, T.; Awe, M.O. Evaluation of Cutting-Tool Coating on the Surface Roughness and Hole Dimensional Tolerances during Drilling of Al6061-T651 Alloy. *Materials* **2021**, *14*, 1783. [CrossRef] [PubMed]
3. Vereschaka, A.; Tabakov, V.; Grigoriev, S.; Sitnikov, N.; Milovich, F.; Andreev, N.; Sotova, C.; Kutina, N. Investigation of the influence of the thickness of nanolayers in wear-resistant layers of Ti-TiN-(Ti,Cr,Al)N coating on destruction in the cutting and wear of carbide cutting tools. *Surf. Coat. Technol.* **2020**, *385*, 125402. [CrossRef]
4. Ll, A.; Qr, A.; Zw, B. Hard and tough CrN coatings strengthened by high-density distorted coherent grain boundaries. *J. Alloy Compd.* **2021**, *894*, 162139.
5. Kao, W.H.; Su, Y.L.; Chung, S.T. Taguchi Optimization of Wear Resistance of CrN Coatings Deposited on WC Substrates Using High-Power Impulse Magnetron Sputtering Technology and Application to High-Speed Micro-Drilling. *J. Mater. Eng. Perform.* **2021**, *30*, 6243. [CrossRef]
6. Ma, Y.; Zhang, K.; Yang, J. Effects of the target-to-substrate distance on the microstructure and properties of TiN coatings fabricated by pulse-enhanced vacuum arc evaporation. *J. Adhes. Sci. Technol.* **2021**, *35*, 1125. [CrossRef]
7. Xian, G.; Xiong, J.; Fan, H.; Jiang, F.; Guo, Z.; Zhao, H.; Xian, L.; Jing, Z.; Liao, J.; Liu, Y. Investigations on microstructure, mechanical and tribological properties of TiN coatings deposited on three different tool materials. *Int. J. Refract. Met. Hard Mater.* **2021**, *102*, 105700. [CrossRef]
8. Baldin, V.; Silva, L.; Baldin, C. Characterization and Performance of TiAlN and TiN Coatings on Plasma-Nitrided AISI 4140 Steel. *Mater. Perform. Charact.* **2021**, *10*, 20200191. [CrossRef]
9. Dong, B.; Mao, T.J.; Chen, W.L. Effects of Al/Cr atom ratios on microstructure and mechanical properties of AlCrTiSiN multi-composite tools coatings. *China Surf. Eng.* **2016**, *29*, 49.
10. Ma, D.Y.; Ma, S.L.; Xu, K.W. The hardess degradation of Ti-Si-N coatings induced by oxygen impurity and its mechanisms. *Chin. J. Mater. Res.* **2008**, *22*, 287.
11. Chen, D.P.; Zhang, P.; Feng, Y. Impacts of Al Content on Mechanical and Tribology Properties of TiAlN Coating. *Tool Eng.* **2016**, *3*, 29.

12. Sun, X.; Li, W.; Huang, J. Effect of Si content on the microstructure and properties of Ti–Si–C composite coatings prepared by reactive plasma spraying. *Ceram. Int.* **2021**, *47*, 24438. [CrossRef]
13. Zhang, W.Y.; Wang, C.M.; Ji, J.X. Synthetic Effect of Cr and Mo Elements on Microstructure and Properties of Laser Cladding NiCrxMoy Alloy Coatings. *Acta Metall. Sin.* **2020**, *33*, 15. [CrossRef]
14. Chang, Y.Y.; Huang, H.L.; Chen, H.J. Antibacterial properties and cytocompatibility of tantalum oxide coatings with different silver content. *Surf. Coat. Technol.* **2014**, *259*, 193. [CrossRef]
15. Ru, Q.; Hu, S.J.; Hu, N.C. Properties of TiAlCrN coatings prepared by vacuum cathodic arc ion plating. *Chin. J. Rare Met.* **2008**, *27*, 251. [CrossRef]
16. Fu, T.C.; Yan, S.J.; Tian, C.X. CrAlTiN and CrAlTiSiN Nanocomposite Coatings Deposited by Multi-arc Plasma Deposition. *China Surf. Eng.* **2013**, *26*, 20.
17. Niu, B.L.; Chen, W.L.; Liu, S.Y. Effects of partial pressure of N2 on microstructure and mechanical properties of AlCrTiSiN superlattice coatings. *China Surf. Eng.* **2015**, *28*, 45.
18. Peng, X.M.; Xia, C.Q.; Wu, A.R. Effect of vacuum heat treatment on microstructure and property of NiCrAlY coating. *Chin. J. Nonferrous Met.* **2013**, *011*, 3147.
19. Bobzin, K.; Brögelmann, T.; Kalscheuer, C. Post-annealing of (Ti,Al,Si)N coatings deposited by high speed physical vapor deposition (HS-PVD). *Surf. Coat. Technol.* **2019**, *375*, 752. [CrossRef]
20. Forsen, R.; Johansson, M.; Oden, M. Decomposition and phase transformation in TiCrAlN thin coatings. *J. Vac. Sci. Technol. A Vac. Surf. Film.* **2012**, *30*, 061506. [CrossRef]
21. Zhang, Z.Q.; Jin, Y.Z.; Chen, C.H. Effects of vacuum heat treatment on properties of TiAlSiN coatings prepared by arc ionplating. *China Surf. Eng.* **2017**, *30*, 70.
22. Flink, A.; Andersson, J.M.; Alling, B. Structure and thermal stability of arc evaporated $(Ti_{0.33}Al_{0.67})_{1-x}Si_xN$ thin films. *Thin Solid Film* **2008**, *517*, 714. [CrossRef]
23. Zhang, S.; Wang, L.; Wang, Q. A superhard CrAlSiN superlattice coating deposited by a multi-arc ion plating: II. Thermal stability and oxidation resistance. *Surf. Coat. Technol.* **2013**, *214*, 153. [CrossRef]
24. Wang, B.; Lu, C.; Sun, C. Effect of NiCrAlY coatings on oxidation resistance of Ni—Base superalloy K17. *Corros. Sci. Prot. Technol.* **2002**, *14*, 7.
25. Geng, D.S.; Wu, Z.T.; Nie, Z.W. Influence of substrate bias on microstructure and thermal stability of AlCrSiON coatings deposited by arc ion plating. *China Surf. Eng.* **2016**, *29*, 60.
26. Wang, L.S.; Liu, X.L.; Zhang, K. Mechanical properties and oxidation resistance of [CrAlSiN/Si$_3$N$_4$]N multilayer coatings. *Met. Funct. Mater.* **2016**, *4*, 17.
27. Chen, Y.S.; Zhang, X.H.; Chen, H.; Liu, H.L. Effect of heat treatment on microstructure and performance of TiAlCeN coating. *Mater. Heat Treat.* **2010**, *39*, 187.
28. Chen, W.; Meng, X.; Wu, D. The effect of vacuum annealing on microstructure, adhesion strength and electrochemical behaviors of multilayered AlCrTiSiN coatings. *Appl. Surf. Sci.* **2019**, *467*, 391. [CrossRef]
29. Ghadami, F.; Aghdam, A.; Ghadami, S. Effect of vacuum heat treatment on the oxidation kinetics of freestanding nanostructured NiCoCrAlY coatings deposited by high-velocity oxy-fuel spraying. *J. Vac. Sci. Technol. A Vac. Surf. Film.* **2020**, *38*, 022601. [CrossRef]
30. Huang, Z.W.; Chang, K.S. Spin-Coating for Fabrication of High-Entropy High-k(AlTiVZrHf)Ox Films on Si for Advanced Gate Stacks. *Ceram. Int.* **2021**, *47*, 9. [CrossRef]
31. Ashith, V.K.; D'Silva, E.D. Influence of concentration and annealing temperature on spin-coated metal oxide thin films for optoelectronic devices. *J. Mater. Sci. Mater. Electron.* **2021**, *32*, 10028. [CrossRef]
32. Meng, D.Q.; Wang, T.G. Influence of vacuum annealing temperature on the structure and properties of AlCrSiN/Mo self-lubricating coatings. *J. Mater. Eng.* **2021**, *49*, 126.
33. Li, Q.Y.; Dong, S.J.; Cao, Q. Thermal stability of multi-layered AlCrN/Cr/AlCrN coatings at elevated temperatures for low thermal emissivity applications. *Appl. Surf. Sci.* **2019**, *498*, 143886. [CrossRef]
34. Sousa, V.F.C.; Da Silva, F.J.G.; Pinto, G.F.; Baptista, A.; Alexandre, R. Characteristics and wear mechanisms of TiAlN-based coatings for machining applications: A comprehensive review. *Metals* **2021**, *11*, 260. [CrossRef]